



## Could negative ion production explain the polar mesosphere winter echo (PMWE) modulation in active HF heating experiments?

A. Kero,<sup>1</sup> C.-F. Enell,<sup>1</sup> A. J. Kavanagh,<sup>2</sup> J. Vierinen,<sup>1</sup> I. Virtanen,<sup>3</sup> and E. Turunen<sup>1</sup>

Received 25 August 2008; revised 2 October 2008; accepted 6 October 2008; published 5 December 2008.

[1] The mechanism behind the modulation of polar mesospheric winter echoes (PMWE) observed in active HF heating experiments is considered. We propose that negative ion chemistry plays a role in the heater-induced modulation of the PMWEs. In the mesosphere, an increased electron temperature leads to a higher rate of electron to neutral attachment, and therefore to a decreased electron density. To a first-order approximation, scattering from Bragg-scale gradients caused by turbulence can be considered to be proportional to the electron density squared. Under this assumption, the electron density variation calculated by the detailed Sodankylä Ion Chemistry model (SIC) predicts correctly both the magnitude and the timescale of the modulation observed with the EISCAT VHF radar. **Citation:** Kero, A., C.-F. Enell, A. J. Kavanagh, J. Vierinen, I. Virtanen, and E. Turunen (2008), Could negative ion production explain the polar mesosphere winter echo (PMWE) modulation in active HF heating experiments?, *Geophys. Res. Lett.*, 35, L23102, doi:10.1029/2008GL035798.

### 1. Introduction

[2] Coherent radar echoes from the mesosphere on both summer and winter periods have become a familiar feature in radar data across a range of latitudes and operating frequencies [e.g., Woodman and Guillen, 1974; Czechowsky et al., 1979; Ecklund and Balsley, 1981; Karashtin et al., 1997; Röttger et al., 1988, 1990]. Over the years much effort has gone into understanding the underlying cause of the so-called polar mesosphere summer echoes (PMSE) [Rapp and Lübken, 2004], including direct stimulation of the ionosphere with powerful high frequency (HF) heaters [e.g., Chilson et al., 2000; Belova et al., 2003]. Results of dedicated active experiments [Havnes et al., 2003] have confirmed the established premise that PMSE relies on the existence of charged aerosol particles in the cold summer mesosphere [von Zahn and Bremer, 1999; Lübken et al., 2002; Havnes et al., 1996]. Careful modeling of the electron temperature dependent charging of the aerosols explains the variation in PMSE power during the heating experiments [e.g., Havnes, 2004].

[3] As mentioned, strong radar returns from the mesosphere are not confined to the polar latitudes. Therefore, the

commonly used concept of polar mesosphere winter echoes (PMWE) is actually a misnomer [e.g., Woodman and Guillen, 1974]. In the high latitudes, PMWE were first observed in the 1980s in Alaska [Ecklund and Balsley, 1981; Balsley et al., 1983] and Norway [Czechowsky et al., 1989]. In each case the mechanism for generating the scatter was determined to be turbulence from breaking gravity waves. PMWE occur at a lower altitude than PMSE (50 to 80 km) [Kirkwood et al., 2002] and against a background of elevated electron density such as during solar proton events [e.g., Collis et al., 1992].

[4] Measurements with lidar and radar [Stebel et al., 2004] have raised questions over the assumption that aerosol particles in the winter hemisphere are too small and too few to influence the radar echoes. As a result for an extensive rocket campaign, Lübken et al. [2006] concluded that characteristics of PMWE can be fully explained by the turbulence alone, without aerosols involved. On the other hand, recent rocket and radar observations show clear evidence for nanometer scale particles throughout the polar winter mesosphere [Strelnikova et al., 2007; Rapp et al., 2008] and hence, the possible role of these particles in the PMWE formation should be reconsidered.

[5] Moreover, a competing explanation over the cause of PMWE has been proposed by Kirkwood et al. [2006]. According to this idea, here referred as viscosity wave theory, the PMWE is caused by scattering from evanescent ion-acoustic waves, i.e., viscosity waves, which are generated by partial reflection of infrasonic waves. Kirkwood [2007] presents two observational contradictions to the traditional turbulence theory, which could be qualitatively explained by the viscosity wave theory. Firstly, a detailed analysis of ESRAD 52 MHz interferometric radar data has shown horizontal velocities of a few hundred meters per second within the PMWE [Kirkwood et al., 2006]. Secondly, by using a typical PMWE observation by the EISCAT VHF radar, Kirkwood [2007] demonstrates that the width of the backscattered spectrum inside the PMWE is equal to the values above and below the layer.

[6] The latter argument has been recently questioned by investigating directly the measured autocorrelation function (ACF), instead of spectra determined as its Fourier transformation. By using the spectral characterization method by Jackel [2000], based on a fitting of a generalized exponential function into the detected ACF, Lübken et al. [2007] show that the spectral shape of the PMWE is, in their case, close to Gaussian and the spectrum above the echo is of Lorentzian shape. This supports strongly the turbulence interpretation of the PMWE.

[7] Since HF heating of the ionosphere has proved to be an important diagnostic technique for PMSE, it has recently been applied to PMWE as well. Kavanagh et al. [2006]

<sup>1</sup>Sodankylä Geophysical Observatory, University of Oulu, Sodankylä, Finland.

<sup>2</sup>Department of Communication Systems, Lancaster University, Lancaster, UK.

<sup>3</sup>Department of Physical Sciences, University of Oulu, Oulu, Finland.

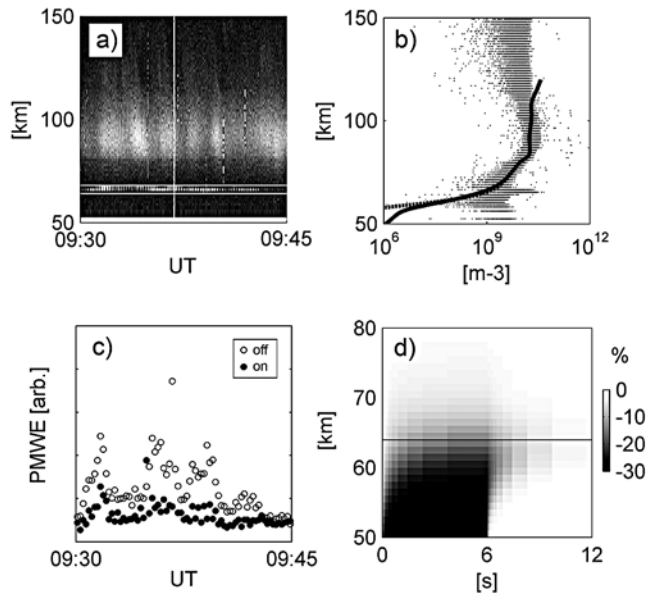


**Figure 1.** (a) Backscattered power detected by the EISCAT VHF radar 24 November 2006. Horizontal solid lines represent the PMWE altitude range (63–66 km). (b) Theoretical incoherent scatter power (dashed line) based on the SIC modeled electron density profile (solid line) versus observed backscatter power (dots). (c) Mean PMWE strength for each of the 6 second heater on/off periods. (d) SIC modeled electron density response to 6 second on/off heating. In this case,  $T_e = 5T_n$  during the on period.

made the first observations of PMWE being modulated by high-power heating; their results demonstrated a distinct effect, similar to the results of *Chilson et al.* [2000] for PMSE. Epoch analysis of a short period heating cycle (10 seconds on and off) showed evidence of a recovery in the PMWE during heater-on. In PMSE experiments this was taken as evidence for the presence of charged aerosols [*Havnes et al.*, 2003]; however the experiment performed by *Kavanagh et al.* [2006] was not optimized for determining this. *Belova et al.* [2008] attempted to repeat the experiment of *Havnes et al.* [2003] for PMWE. They concluded that a so-called overshoot effect, i.e., a sudden increase of the echo power above the original level after the heater was turned off, was present, perhaps indicating the presence of very small dust particles. However, they acknowledged the need for better statistics before drawing firm conclusions.

[8] In this paper we present one EISCAT VHF incoherent scatter radar (224 MHz) observation of PMWE modulation induced by the EISCAT Heating facility. We interpret the characteristics of the data in terms of mesospheric ion chemistry using the Sodankylä Ion Chemistry (SIC) model. We suggest an electron temperature dependent negative ion production as a possible mechanism participating to the heating-induced PMWE modulation.

## 2. Data

[9] In November 2006, a set of EISCAT heating experiments were carried out dedicated to detect the D-region heating effect by using newly designed methods for the

VHF radar [*Kero et al.*, 2008]. In this study we focus on the first of the six data examples (Figure 1a). In this particular case, the overall heating signature in the incoherent scatter, above the altitudes of a strong PMWE, was the weakest of all 6 data examples. In contrast, the backscattered power from the PMWE modulated clearly along the heating cycle (Figure 1c). In order to characterize the origin of the backscatter in different heights, we adopted the method presented by *Jackel* [2000]. A generalized exponential function of form  $a(\tau) = A \exp(iB\tau - (C\tau)^n)$  was fitted to the detected ACF by using  $A$ ,  $B$ ,  $C$  and  $n$  as free parameters. In particular, at the altitude of the PMWE, the  $n$ -parameter was found to be close to 2 ( $n = 1.91 \pm 0.09$ ), which indicates a Gaussian spectral shape. This confirms the result by *Lübken et al.* [2007] indicating that the PMWE is caused by scattering from turbulence. Above the PMWE, the  $n$ -parameter decays close to unity ( $n = 1.06 \pm 0.08$  at 80 km), which corresponds to Lorentzian shaped spectrum of incoherent scattering. In fact, the  $n$ -parameter stays consistently above 1 throughout the D-region altitudes, which according to diagnostics proposed by *Rapp et al.* [2007], may indicate an absence of dust particles in our case.

[10] The super-imposed epoch analysis (SEA) shown in Figure 2 reveals the characteristic PMWE response to the HF heating. In this approach, the PMWE power was divided in super-imposed sequences according to the 6 second on/off heating cycles. In order to obtain the relative PMWE power change during the cycles, each sequence was normalized by the PMWE power corresponding to the end of the current and previous cycle (mean value of the first and the last column in Figure 2). Distributions of the SEA

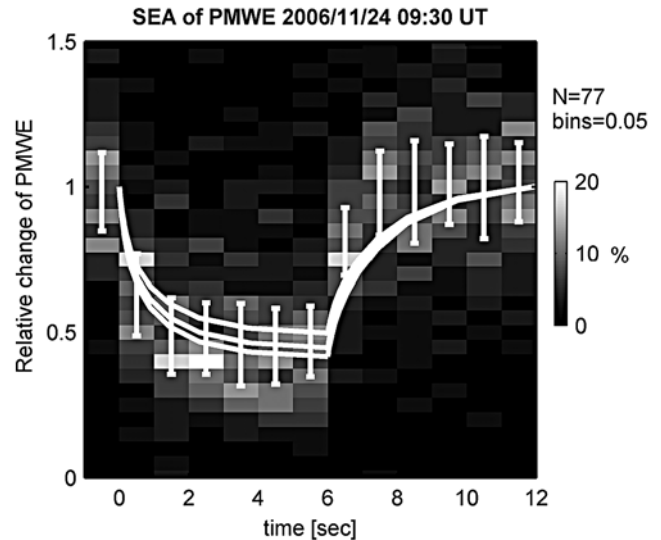


**Figure 2.** Superimposed Epoch Analysis (SEA) of the PMWE strength and SIC modeled change of  $N_e^2$ . The distributions of the 77 superimposed PMWE strength estimates are illustrated as vertical gray scale histograms. The error bars represent the limits of the 50 percent centermost SEA estimates. The solid lines show the SIC modeled  $N_e^2$  response to the 6 second on/off heating corresponding to electron-neutral temperature ratios of 5 (upper line), 10 (middle) and 30 (lower) during the on period.

**Table 1.** List of the Prominent Reactions Causing the Heating-Induced Electron Density Modulation in SIC 7.2<sup>a</sup>

Reaction	Rate Coefficient
a) $2\text{O}_2 + e \rightarrow \text{O}_2^- + \text{O}_2$	$4 \times 10^{-30} \times \exp(-193/T_e)$
b) $\text{O}_2^- + \text{O}_2 + \text{M} \rightarrow \text{O}_4^- + \text{M}$	$3.4 \times 10^{-31}$
c) $\text{O}_4^- + \text{CO}_2 \rightarrow \text{CO}_4^- + \text{O}_2$	$4.3 \times 10^{-10}$
d) $\text{CO}_4^- + \text{O} \rightarrow \text{CO}_3^- + \text{O}_2$	$1.4 \times 10^{-10}$
e) $\text{CO}_3^- + \text{O} \rightarrow \text{O}_2^- + \text{CO}_2$	$1.1 \times 10^{-10}$
f) $\text{O}_2^- + \text{O}_2(^1\Delta_g) \rightarrow 2\text{O}_2 + e$	$2 \times 10^{-10}$

<sup>a</sup>Following the original scheme of *Turunen et al.* [1996]. The unit of the rate coefficient for the three-body reactions a) and b) is  $\text{cm}^6\text{s}^{-1}$  and for the rest it is  $\text{cm}^3\text{s}^{-1}$ . The electron temperature  $T_e$  is given in Kelvins.

estimates along the heating cycle are illustrated in Figure 2 as vertical gray scale histograms. In addition, error bars show the limits of 50% centermost points in the distributions.

[11] The analysis shows that the PMWE strength is reduced approximately to half the background level after the heater is turned on, and when turned off, the echo power recovers to the original level. Both these transitions take approximately two seconds, which are several orders of magnitude longer timescales than typical transition times in the PMSE modulation [*Belova et al.*, 2003]. Moreover, neither an overshoot effect after the heater is turned off, nor a recovery during the heater-on period was found in the analysis. The absence of these characteristics, typically associated with the PMSE modulation, may be due to the 6 seconds on/off modulation used in the experiment being too fast. The chosen modulation provides, however, a relatively good statistical sample of SEA estimates, and therefore reveals clearly the characteristics of the PMWE modulation.

### 3. Model

[12] The electron density response to the HF heating was parameterized by *Kero et al.* [2008] by using the Sodankylä Ion Chemistry model (SIC) [*Verronen*, 2006] extended version 7.2 which solves the concentrations of 36 positive ions, 29 negative ions and 15 minor neutrals via 339 reactions [*Enell et al.*, 2005]. It should be noted that the negative ion chemistry of the SIC 7.2 is updated to include a revision according to *Kazil et al.* [2003]. Before the parametrization of the chemistry response to the heating, the model was preconditioned to reproduce the EISCAT VHF background power profile (see Figure 1b) by introducing solar radiation [*Tobiska et al.*, 2000] and an adjusted electron precipitation as ionization sources.

[13] Here, the chemical response to the 6 second on/off heating at the PMWE altitude is studied for the electron temperatures  $T_e$  increased during the heater-on periods by a factor of 5, 10 and 30 above the neutral temperature  $T_n$  of 240 K (MSISE-90 model) [*Hedin*, 1991]. The SIC model predicts that the electron temperature increase leads to a higher electron attachment rate, i.e., production of negative ions, and therefore to a loss of free electrons (see Figure 1d). The electron density reduction reaches its saturation point during the heater-on period, and recovers to the background state during the off period, in time-scales of few seconds.

[14] Table 1 lists the most important reactions responsible for the electron density modulation. The primary negative

ion  $\text{O}_2^-$  is produced via the electron temperature dependent attachment process (a). The following reactions in the chain (b, c and d) transfer  $\text{O}_2^-$  ions effectively into  $\text{CO}_4^-$  and  $\text{CO}_3^-$ . In the end of the heating period only 32 percent of the electron density decrease is due to  $\text{O}_2^-$ , while  $\text{CO}_4^-$  and  $\text{CO}_3^-$  correspond to 22 and 46 percents respectively. The loss reaction chain (e and f) leads to saturation during the heater-on period, and recovery when the heater is turned off. Under the assumption that the backscattered power from the PMWE is proportional to the electron density squared [*Lübken et al.*, 2006], the modeled response, i.e., the relative change of  $N_e^2$ , can be compared to the observed PMWE modulation. In Figure 2, the modeled curves correspond to the heating factors of 5, 10 and 30.

### 4. Discussion

[15] Figure 2 shows that the electron temperature dependent negative ion chemistry offers a potential explanation for the HF heating induced PMWE modulation with reasonable electron heating factors. Besides the magnitude, the timescale of the modeled PMWE response matches the observed one well. The model predicts only a slightly slower PMWE response compared to the median behavior of the superimposed PMWE observations. This small difference, however, can be due to uncertainties in the model preconditioning (see Figure 1b) which has an effect on the characteristic electron density response. Note that the model is not re-adjusted to match the data for this particular application. The chemistry parametrization presented in this paper is the same as shown by *Kero et al.* [2008], where the effect of the heating dependent chemistry on the incoherent scatter spectrum was studied.

[16] The critical assumption that the PMWE power is proportional to the electron density squared, must be regarded as a first order approximation of the true turbulence scattering response to the heating. Appendix A of *Rapp et al.* [2008] shows in details the derivation of the turbulence scattering cross section for stationary conditions, where the production of small scale gradients by turbulence is balanced by the diffusion. A challenge for the work in future would be to develop a time-dependent model describing the turbulence scattering in non-stationary conditions, where the electron temperature changes both the chemistry and the diffusion of the plasma. Moreover, the chemistry scheme should be upgraded to include the recently observed charged dust particles in order to quantify their contribution to the PMWE modulation.

### 5. Conclusions

[17] The electron temperature dependent negative ion chemistry offers a potential explanation for the observed PMWE modulation shown in Figure 2, assumed that the echo power is proportional to the electron density squared. The ion chemistry, which is responsible for most of the electron density changes in the model, follows the reaction chain listed in Table 1. Besides the need of further PMWE observations during heating experiments, a non-stationary theory for the turbulence backscattering should be developed for more realistic diagnostics of the heating induced PMWE modulation. This work indicates that the D-region

negative ion chemistry should be taken into account in this approach.

[18] **Acknowledgments.** The main author's work is funded by the Academy of Finland research project 123275, THERMES. Juha Vierinen is funded by the Academy of Finland (application 213476, Finnish Programme for Centres of Excellence in Research 2006-2011). Carl-Fredrik Enell is funded by the Academy of Finland through project 109054, Solar Energetic Radiation and Chemical Aeronomy of the Mesosphere. Ilkka Virtanen is funded by the Finnish Graduate School in Astronomy and Space Physics. A. J. Kavanagh was supported by the LAPBIAT2 program (contract RITA-CT-2006-025969). The EISCAT measurements were made with special programme time granted for Finland. EISCAT is an international association supported by China (CRIRP), Finland (SA), Germany (DFG), Japan (STEL and NIPR), Norway (NFR), Sweden (VR) and United Kingdom (STFC).

## References

- Balsley, B. B., W. L. Ecklund, and D. C. Fritts (1983), VHF echoes from the high-latitude mesosphere and lower thermosphere, observations and interpretations, *J. Atmos. Sci.*, *40*, 2451–2466.
- Belova, E., P. B. Chilson, S. Kirkwood, and M. T. Rietveld (2003), Response time of PMSE to ionospheric heating, *J. Geophys. Res.*, *108*(D8), 8446, doi:10.1029/2002JD002385.
- Belova, E., M. Smirnova, M. T. Rietveld, B. Isham, S. Kirkwood, and T. Sergienko (2008), First observation of the overshoot effect for polar mesosphere winter echoes during radiowave electron temperature modulation, *Geophys. Res. Lett.*, *35*, L03110, doi:10.1029/2007GL032457.
- Chilson, P. B., E. Belova, M. T. Rietveld, S. Kirkwood, and U.-P. Hoppe (2000), First artificially induced modulation of PMSE using the EISCAT heating facility, *Geophys. Res. Lett.*, *27*, 3801–3804.
- Collis, P. N., M. T. Rietveld, J. Röttger, and W. K. Hocking (1992), Turbulence scattering layers in the middle-mesosphere observed by the EISCAT 224-MHz radar, *Radio Sci.*, *27*, 97–107.
- Czechowsky, P., R. Rüster, and G. Schmidt (1979), Variations of mesospheric structures in different seasons, *Geophys. Res. Lett.*, *6*, 459–462.
- Czechowsky, P., I. M. Reid, R. Rüster, and G. Schmidt (1989), VHF radar echoes observed in the summer and winter polar mesosphere over Andøya, Norway, *J. Geophys. Res.*, *94*, 5199–5217.
- Ecklund, W. L., and B. B. Balsley (1981), Long-term observations of the Arctic mesosphere with the MST radar at Poker Flat, Alaska, *J. Geophys. Res.*, *86*, 7775–7780.
- Enell, C.-F., A. Kero, E. Turunen, T. Ulich, P. T. Verronen, A. Seppälä, S. Marple, F. Honary, and A. Senior (2005), Effects of D-region RF heating studied with the Sodankylä Ion Chemistry model, *Ann. Geophys.*, *23*, 1575–1583.
- Havnes, O. (2004), Polar Mesospheric Summer Echoes (PMSE) overshoot effect due to cycling of artificial electron heating, *J. Geophys. Res.*, *109*, A02309, doi:10.1029/2003JA010159.
- Havnes, O., J. Trøim, T. Blix, W. Mortensen, L. I. Næsheim, E. Thrane, and T. Tønnesen (1996), First detection of charged dust particles in the Earth's mesosphere, *J. Geophys. Res.*, *101*, 10,839–10,847.
- Havnes, O., C. La Hoz, L. I. Næsheim, and M. T. Rietveld (2003), First observations of the PMSE overshoot effect and its use for investigating the conditions in the summer mesosphere, *Geophys. Res. Lett.*, *30*(23), 2229, doi:10.1029/2003GL018429.
- Hedin, A. E. (1991), Extension of the MSIS thermosphere model into the middle and lower atmosphere, *J. Geophys. Res.*, *96*, 1159–1172.
- Jackel, B. J. (2000), Characterization of auroral radar power spectra and autocorrelation functions, *Radio Sci.*, *35*, 1009–1023.
- Karashin, A. N., Y. V. Shlyugaev, V. I. Abramov, I. F. Belov, I. V. Berezin, V. V. Bychkov, E. B. Eryshev, and G. P. Komrakov (1997), First HF radar measurements of summer mesopause echoes at SURA, *Ann. Geophys.*, *15*, 935–941.
- Kavanagh, A. J., F. Honary, M. T. Rietveld, and A. Senior (2006), First observations of the artificial modulation of polar mesospheric winter echoes, *Geophys. Res. Lett.*, *33*, L19801, doi:10.1029/2006GL027565.
- Kazil, J., E. Kopp, S. Chabrilat, and J. Bishop (2003), The University of Bern Atmospheric Ion Model: Time-dependent modeling of the ions in the mesosphere and lower thermosphere, *J. Geophys. Res.*, *108*(D14), 4432, doi:10.1029/2002JD003024.
- Kero, A., J. Vierinen, C.-F. Enell, I. Virtanen, and E. Turunen (2008), New incoherent scatter diagnostic methods for the heated D-region ionosphere, *Ann. Geophys.*, *26*, 2273–2279.
- Kirkwood, S. (2007), Polar mesosphere winter echoes—A review of recent results, *Adv. Space Res.*, *40*, 751–757.
- Kirkwood, S., V. Barabash, E. Belova, H. Nilsson, T. N. Rao, K. Stebel, A. Osepian, and P. B. Chilson (2002), Polar mesosphere winter echoes during solar proton events, *Adv. Polar Upper Atmos. Res.*, *16*, 111–125.
- Kirkwood, S., P. Chilson, E. Belova, P. Dalin, I. Häggström, M. Rietveld, and W. Singer (2006), Infrasound—The cause of strong polar mesosphere winter echoes?, *Ann. Geophys.*, *24*, 475–491.
- Lübken, F., M. Rapp, and P. Hoffmann (2002), Neutral air turbulence and temperatures in the vicinity of polar mesosphere summer echoes, *J. Geophys. Res.*, *107*(D15), 4273, doi:10.1029/2001JD000915.
- Lübken, F.-J., B. Strelnikov, M. Rapp, W. Singer, R. Latteck, A. Brattli, U.-P. Hoppe, and M. Friedrich (2006), The thermal and dynamical state of the atmosphere during polar mesosphere winter echoes, *Atmos. Chem. Phys.*, *6*, 13–24.
- Lübken, F., W. Singer, R. Latteck, and I. Strelnikova (2007), Radar measurements of turbulence, electron densities, and absolute reflectivities during polar mesosphere winter echoes (PMWE), *Adv. Space Res.*, *40*, 758–764.
- Rapp, M., and F.-J. Lübken (2004), Polar mesosphere summer echoes (PMSE): Review of observations and current understanding, *Atmos. Chem. Phys.*, *4*, 2601–2633.
- Rapp, M., I. Strelnikova, and J. Gumbel (2007), Meteoric smoke particles: Evidence from rocket and radar techniques, *Adv. Space Res.*, *40*, 809–817.
- Rapp, M., I. Strelnikova, R. Latteck, P. Hoffmann, U.-P. Hoppe, I. Häggström, and M. T. Rietveld (2008), Polar mesosphere summer echoes (PMSE) studied at Bragg wavelengths of 2.8 m, 67 cm, and 16 cm, *J. Atmos. Sol. Terr. Phys.*, *70*, 947–961.
- Röttger, J., C. La Hoz, M. C. Kelley, U.-P. Hoppe, and C. Hall (1988), The structure and dynamics of polar mesosphere summer echoes observed with the EISCAT 224 MHz radar, *Geophys. Res. Lett.*, *15*, 1353–1356.
- Röttger, J., M. T. Rietveld, C. La Hoz, T. Hall, M. C. Kelley, and W. E. Swartz (1990), Polar mesosphere summer echoes observed with the EISCAT 933-MHz radar and the CUPRI 46.9-MHz radar, their similarity to 224-MHz radar echoes, and their relation to turbulence and electron density profiles, *Radio Sci.*, *25*, 671–687.
- Stebel, K., U. Blum, K.-H. Fricke, S. Kirkwood, N. Mitchell, and A. Osepian (2004), Joint radar/lidar observations of possible aerosol layers in the winter mesosphere, *J. Atmos. Sol. Terr. Phys.*, *66*, 957–970.
- Strelnikova, I., M. Rapp, S. Raizada, and M. Sulzer (2007), Meteor smoke particle properties derived from Arecibo incoherent scatter radar observations, *Geophys. Res. Lett.*, *34*, L15815, doi:10.1029/2007GL030635.
- Tobiska, W., T. Woods, F. Eparvier, R. Viereck, L. Floyd, D. Bouwer, G. Rottman, and O. White (2000), The SOLAR2000 empirical solar irradiance model and forecast tool, *J. Atmos. Sol. Terr. Phys.*, *62*, 1233–1250.
- Turunen, E., H. Matveinen, J. Tolvanen, and H. Ranta (1996), D-Region ion chemistry model, in *STEP Handbook of Ionospheric Models*, edited by R. W. Schunk, pp. 1–25, Sci. Comm. on Sol. Terr. Phys., Boulder, Colo.
- Verronen, P. T. (2006), Ionosphere-atmosphere interaction during solar proton events, Ph.D. thesis, Finn. Meteorol. Inst., Helsinki.
- von Zahn, U., and J. Bremer (1999), Simultaneous and common-volume observations of noctilucent clouds and polar mesosphere summer echoes, *Geophys. Res. Lett.*, *26*, 1521–1524.
- Woodman, R. F., and A. Guillen (1974), Radar observations of winds and turbulence in the stratosphere and mesosphere, *J. Atmos. Sci.*, *31*, 493–505.
- C.-F. Enell, A. Kero, E. Turunen, and J. Vierinen, Sodankylä Geophysical Observatory, University of Oulu, Tähteläntie 62, FIN-99600 Sodankylä, Finland. (antti.kero@sgo.fi)
- A. J. Kavanagh, Department of Communication Systems, Lancaster University, Infolab 21, Lancaster LA1 4YW, UK.
- I. Virtanen, Department of Physical Sciences, University of Oulu, P.O. Box 3000, FIN-90014 Oulu, Finland.